Available online at www.sciencedirect.com

ScienceDirect

Journal of Nutritional Biochemistry 25 (2014) 1243–1253

Journal of Nutritional Biochemistry

Protein carbonylation associated to high-fat, high-sucrose diet and its metabolic effects

Lucía Méndez[a,*], Manuel Pazos[a], Eunice Molinar-Toribio[b], Vanesa Sánchez-Martos[c], José M. Gallardo[a], M. Rosa Nogués[c], Josep L. Torres[b], Isabel Medina[a]

[a]Instituto de Investigaciones Marinas, Consejo Superior de Investigaciones Científicas (IIM-CSIC), E-36208 Vigo, Spain
[b]Instituto de Química Avanzada de Catalunya, Consejo Superior de Investigaciones Científicas (IQAC-CSIC), E-08034 Barcelona, Spain
[c]Unidad de Farmacología. Facultad de Medicina y Ciencias de la Salud, Universidad Rovira i Virgili, E-43201 Reus, Spain

Received 20 December 2013; received in revised form 19 June 2014; accepted 26 June 2014

Abstract

The present research draws a map of the characteristic carbonylation of proteins in rats fed high-caloric diets with the aim of providing a new insight of the pathogenesis of metabolic diseases derived from the high consumption of fat and refined carbohydrates. Protein carbonylation was analyzed in plasma, liver and skeletal muscle of Sprague–Dawley rats fed a high-fat, high-sucrose (HFHS) diet by a proteomics approach based on carbonyl-specific fluorescence-labeling, gel electrophoresis and mass spectrometry. Oxidized proteins along with specific sites of oxidative damage were identified and discussed to illustrate the consequences of protein oxidation. The results indicated that long-term HFHS consumption increased protein oxidation in plasma and liver; meanwhile, protein carbonyls from skeletal muscle did not change. The increment of carbonylation by HFHS diet was singularly selective on specific target proteins: albumin from plasma and liver, and hepatic proteins such as mitochondrial carbamoyl-phosphate synthase (ammonia), mitochondrial aldehyde dehydrogenase, argininosuccinate synthetase, regucalcin, mitochondrial adenosine triphosphate synthase subunit beta, actin cytoplasmic 1 and mitochondrial glutamate dehydrogenase 1. The possible consequences that these specific protein carbonylations have on the excessive weight gain, insulin resistance and nonalcoholic fatty liver disease resulting from HFHS diet consumption are discussed.

Keywords: High-fat, high-sucrose diet; Obesity; Insulin resistance; NAFLD; Protein carbonylation; Sprague–Dawley rat

1. Introduction

Protein carbonylation constitutes the most common biomarker of oxidative protein damage and can be induced by the attack of reactive oxygen species (ROS) [1]. The consumption of high-caloric diets associated to a westernized lifestyle has been linked to the generation of an excess of ROS, particularly superoxide anion through the mitochondrial electron-transport chain, and to the development of multiple metabolic disorders such as obesity, hypertension, hyperglycemia, hyperinsulinemia or dyslipidemia [2–4]. As a consequence of this ROS overproduction, increased protein carbonylation levels have been described occurring together with these diet-induced disorders [5,6].

Protein carbonylation is an irreversible oxidative posttranslational modification, although cells exhibit native enzymatic systems that eliminate altered proteins and maintain cellular homeostasis and survival. These damage response systems are typically proteasome in the cytosol and adenosine triphosphate (ATP)-dependent proteases in mitochondria [7]. When these enzymatic systems come to fail, carbonylated proteins accumulate in the cell, and cellular functions are disrupted because carbonylated proteins either lose their catalytic and structural integrity, or interrupt regulatory pathways [8].

Protein oxidative damage has been traditionally accepted to be a random process since ROS generally attack protein nonenzymatically and radical species such as hydroxyl radicals are so reactive that are they able to oxidize most amino acids [9]. However, several studies have revealed that protein carbonylation is highly selective in diseases such as Alzheimer [10] or uremia [11], or even during the natural aging process. A dietary intervention study of Wistar rats supplemented with fish oils also showed such specificity by down-regulating carbonylation of several plasma and liver proteins [12]. However, to date, few studies have addressed protein oxidation linked to metabolic disorders induced by diet high in fat and/or sugars, and those that exist performed essentially total protein carbonylation measurements [13–17].

The aim of the present study is to evaluate comprehensively the impact of oxidative stress triggered by high-fat, high-sucrose (HFHS) diets on irreversible oxidative protein damage and, particularly, on protein carbonylation. Recent investigations indicated that obesity and insulin resistance are accompanied by an increased carbonylation of certain adipose-regulatory proteins [6,18]. The present work is

* Corresponding author. Tel.: +34 986 231930; fax: +34 986 292762.
E-mail address: luciamendez@iim.csic.es (L. Méndez).

http://dx.doi.org/10.1016/j.jnutbio.2014.06.014
0955-2863/

focused on the explicit carbonylation of plasma, liver and skeletal muscle proteins since these tissues play a key role in the development of metabolic disorders [19], and they have not been addressed before. To this purpose, we analyzed total and individual protein carbonylation in plasma, liver and skeletal muscle from rats fed a HFHS diet for 22 weeks compared with control rats fed a low-fat diet. Proteins susceptible to oxidation and carbonylation sites were identified by using a proteomics approach based on gel electrophoresis and protein identification by tandem mass spectrometry (MS/MS). Protein carbonylation was correlated with morphological measurements, and biochemical parameters of lipid and carbohydrate metabolism, lipid peroxidation products and endogenous antioxidant systems, and discussed in terms of its potential implication on the metabolic disorders observed.

2. Materials and methods

2.1. Materials and reagents

Fluorescein-5-thiosemicarbazide (FTSC) was purchased from Invitrogen (Carlsbad, CA), and porcine sequencing-grade modified trypsin was from Promega (Madison, WI). Ketamine chlorhydrate (Imalgene 1000) was purchased from Merial Laboratorios S.A. (Barcelona, Spain), and xylacine (Rompun 2%) was from Quimica Farmaceutica S.A. (Barcelona, Spain). ProteoBlock protease inhibitor cocktail was purchased from Thermo Fisher Scientific Inc. (Rockford, IL). Phenylmethylsulfonyl fluoride (PMSF); dithiothreitol (DTT); iodoacetamide; ethylenediaminetetraacetic acid (EDTA); trichloroacetic acid (TCA); Tris–HCl; 3,3-cholaminopropyl-dimethylammonio-1-propanesulfonate (CHAPS); sodium phosphate; magnesium chloride anhydrous; 2,2 -azobis(2-amidinopropane) dihydrochloride (AAPH); 3 ,6 -dihydroxyspiro[isobenzofuran-1[3H],9 [9H]-xanthen]-3-one (fluorescein); 6-hydroxy-2,5,7,8-tetramethylchroman-2-carboxylic acid (Trolox); 2-thiobarbituric acid; 1,1,3,3,-tetraethoxypropane; propyl gallate and bicinchoninic acid (BCA) were purchased from Sigma-Aldrich (St. Louis, MO). Urea, thiourea, sodium dodecyl sulfate (SDS), glycine, glycerol and Serdolit MB-1 were obtained from USB (Cleveland, OH). IPG buffer; Pharmalyte 3–10; ammonium persulfate; bromophenol blue; and 1,2-bis(dimethylamino)ethane were purchased from GE Healthcare Science (Uppsala, Sweden). Acrylamide; bis-*N,N* -methylene-bis-acrylamide; and Bio-Rad protein assay were obtained from Bio-Rad (Hercules, CA). All other chemicals and reagents used were of analytical reagent grade, and water was purified using a Milli-Q system (Millipore, Billerica, MA).

2.2. Animals and experimental design

Male 22-week-old Sprague–Dawley rats weighing between 500 and 600 g (Janvier, Le Genest-St-Isle, France) were housed in animal cages (n=2–3/cage) with constantly regulated temperature (22°C±2°C), humidity (50%±10%) and light-controlled room (lights on 06:30–18:30). The animals were randomly assigned to one of two dietary groups: a control group (n=5) fed the reference diet Teklad Global 2014 (Harlan Teklad Inc., Indianapolis, IN) and a group (n=5) fed a HFHS based on TD. 08811 diet (Harlan Teklad Inc.). Rats had *ad libitum* access to water and food. Food intake and water consumption were registered daily throughout the study (means are shown in Table 1). After 22 weeks of experiment, rats were fasted overnight, anesthetized intraperitoneally with ketamine and xylacine (80 mg/kg and 10 mg/kg body weight, respectively) and then killed by exsanguination. The control diet composition was (% by weight) 4.3% fat (3.9% soybean oil), 46.7% available carbohydrate (41% corn and wheat starches), 16.3% protein, 21.5% total fiber, 4.6% minerals and 1.2% vitamins. Fats provided 13.3% of calories, carbohydrates provided 64.3%, and proteins provided 22.5%. Total energy density was 2.9 kcal/g. HFHS diet composition was (% by weight) 24.3% fat (21% anhydrous milk fat, 2% soybean oil), 43.5% available carbohydrate (32.4% sucrose), 20.9% protein, 4.7% total fiber (from cellulose), 4.1% minerals, 1.8% vitamins (from American Institute of Nutrition 93-VX (94047)) and 0.004% antioxidants. Fats provided 45.9% of calories, carbohydrates provided 36.5% (27% from sucrose), and proteins provided 17.6%. Total energy density was 4.7 kcal/g. The approximate fatty acid profile of control diet (% of total fat) was 18% saturated fatty acids (SFA), 20% monounsaturated fatty acids (MFA) and 62% polyunsaturated fatty acids (PUFA). In the HFHS diet, the fatty acid profile was 61% SFA, 31% MUFA and 8% PUFA. The HFHS diet contained about 0.05% of cholesterol, mainly from the anhydrous milk fat. Control diet can contain small amounts of cholesterol, likely less than 0.001%. All the procedures followed the European Union guidelines for the care and management of laboratory animals, and all efforts were made to minimize suffering. The pertinent permission for this specific study was obtained from the CSIC (Spanish Research Council) Subcommittee of Bioethical Issues (ref. AGL2009-12 374-C03-03).

2.3. Sample collection

Total abdominal fat, corresponding to the sum of epididymal, perirenal and mesenteric depots, liver and skeletal muscle from hind leg were excised, washed with 0.9% NaCl solution, weighed and immediately frozen in liquid nitrogen upon sacrifice.

Table 1
Body measurements and metabolic variables in rats

		Control (n=5)	HFHS (n=5)
Final body weight (g)		722.4 (95.6)	918.2 (93.3) *
Food intake (g/day)		26.7 (1.2)	21.9 (0.5) *
Energy intake (kcal/day)		77.4 (8.8)	101.0 (8.4) *
Total abdominal fat weight (g)		32.4 (13.8)	60.7 (9.3) **
Adiposity index (%) [a]		4.4 (1.2)	6.7 (1.5) *
Liver weight (g)		15.6 (3.6)	24.8 (6.8) *
Total liver lipids (mg/g)		2.3 (0.2)	8.8 (1.9) **
Hepatosomatic index (%) [b]		2.1 (0.3)	2.7 (0.8)
Total cholesterol (mmol/L)		2.87 (0.40)	2.26 (0.20)
LDL-C (mmol/L)		0.42 (0.11)	0.29 (0.04)
HDL-C (mmol/L)		0.73 (0.06)	0.60 (0.06)
Triglycerides (mmol/L)		2.13 (0.34)	1.71 (0.33)
HbA1c (%)		5.7 (0.4)	5.0 (0.1)
Plasma glucose (mmol/L)		4.1 (0.4)	4.5 (0.5)
Plasma insulin (pmol/L)	Week 5	0.25 (0.10)	1.16 (0.11) **
	Week 9	0.27 (0.12)	0.80 (0.03) **
	Week 13	0.29 (0.14)	0.88 (0.05) **

Results are means (standard deviation); n, number of rats.
[a] Adiposity index: (total abdominal fat×100)/body weight.
[b] Hepatosomatic index: (liver weight×100)/body weight.
* P<.05 vs. control group.
** P<.01 vs. control group.

The adiposity index [(total abdominal fat×100)/body weight] and hepatosomatic index [(liver weight×100)/body weight] were determined. One part of dissected livers was used for histological analysis. Blood samples were collected on a tube with EDTA by cardiac puncture, and plasma and erythrocyte samples were separated by centrifugation (850*g*, 4°C, 15min). Plasma samples for protein oxidation measurement were supplemented with 5 mM PMSF. All samples were stored at −80°C until analysis.

2.4. Biochemical measurements

Triglycerides, cholesterol, low-density lipoprotein (LDL) cholesterol and high-density lipoprotein (HDL) cholesterol were measured by spectrophotometric methods (SpinReact Kits, Girona, Spain) [20,21]. The percentage of glycated hemoglobin, or HbA1c, in the blood was determined according to Sharp et al. [22]. Blood glucose levels were measured by an enzyme electrode method using the Ascensia ELITE XL blood glucose meter (Bayer Consumer Care AG, Basel, Switzerland). Plasma insulin concentrations were measured using a Rat/Mouse Insulin ELISA kit according to the manufacturer's instructions (Millipore Corporation, Billerica, MA).

2.5. Determination of lipid peroxidation levels and antioxidant systems in blood and liver samples

For estimating lipid peroxidation levels, we measured three different products of lipid peroxidation: lipid hydroperoxides (primary lipid oxidation product), conjugated dienes (intermediate oxidation product) and malondialdehyde (MDA) (end oxidation product). The first step for the estimation of lipid hydroperoxides and conjugated dienes was to extract liver lipids with dichloromethane [23] and to determine total lipid content [24]. Then, conjugated dienes were measured following the American Oil Chemists' Society method [25], and lipid hydroperoxides were measured following the method of Chapman and Mackay [26]. We also measured total MDA concentrations in plasma and liver. Total MDA was derivatized with thiobarbituric acid (TBA) after protein hydrolysis [27] and precipitation [28], and determined by high-performance liquid chromatography fluorescence according to Fukunaga et al. [29]. Total superoxide dismutase (SOD) activity was measured in plasma and liver following the method of Misra and Fridovich [30]. Catalase (CAT) activity was measured in plasma and liver according to the procedure of Cohen et al. [31]. Glutathione peroxidase (Gpx) and glutathione reductase (GR) activities were determined according to Wheeler et al. [32]. The oxidized and reduced glutathione balance (GSSG/GSH) was measured by the Hissin and Hilf fluorometric method [33]. The oxygen radical absorbance capacity (ORAC) from plasma and liver was determined according to Ou et al. [34]. ORAC measures antioxidant scavenging activity against peroxyl radicals induced by AAPH using fluorescein as fluorescent probe and Trolox as standard and quality control.

2.6. Liver histological studies

Livers fixed in formalin were dehydrated in alcohol and embedded in paraffin. Serial liver sections (3 μm) were stained with haematoxylin/eosin (Harris Hematoxylin, Química Clínica Aplicada, S.A., Tarragona, Spain). Liver injury such as steatosis, lobular inflammation and fibrosis was evaluated by histological examination under a light microscope, as previously described [35]. Briefly, ten 200× light microscopic fields were viewed on each section and scored for the severity of hepatic steatosis, inflammation and fibrosis according to the following criteria: for hepatic steatosis (expressed as percent of

hepatocytes containing fat droplets): grade 0, no fat; grade 1, steatosis occupying less than 33% of the hepatic parenchyma; grade 2, 34%–66% of the hepatic parenchyma; grade 3, more than 66% of the hepatic parenchyma; for inflammatory cell infiltration (graded on the basis of the presence of inflammatory cells): grade 0: none; grade 1, 1–2 foci/field; grade 2, 3–4 foci/field; grade 3, more than 4 foci/field. The staging of hepatic fibrosis was investigated as follows: 0, none; 1, mild, zone 3, perisinusoidal; 2, moderate, zone 3, perisinusoidal; 3, portal/periportal; 4, bridging fibrosis.

2.7. Protein extraction and fractionation

To reduce sample complexity, proteins from liver and skeletal muscle were fractioned according to hydrophobicity into proteins soluble at low ionic strength (LIS fraction), mostly water-soluble proteins, and proteins soluble at high ionic strength (HIS fraction), mostly containing hydrophobic proteins associated with the various membranes in the cell. This sample fractionation improves sensitivity of water-soluble low abundance proteins. Between 200 and 400 mg of either liver or muscle was homogenized with an Ultra-Turrax high-performance disperser, in 25 vol of 20 mM sodium phosphate, pH 6.0, 0.5 mM $MgCl_2$, 1 mM EDTA and 10-μl/ml buffer of ProteoBlock protease inhibitor cocktail (100 mM AEBSF HCl, 80 μM aprotinin, 5 mM bestatin, 1.5 mM E64, 2 mM leupeptin and 1 mM pepstatin A). Homogenized samples were centrifuged at 100,000*g* for 1 h at 4°C, and LIS fraction was recovered in the supernatants. HIS fraction was isolated by homogenization of the remaining pellets in 10 vol of 10 mM Tris–HCl, pH 7.2, 0.6 M NaCl, 1 mM EDTA and 10-μl/ml buffer of ProteoBlock protease inhibitor cocktail. After centrifugation at 16,000*g* for 15 min at 4°C, HIS fractions were contained in the supernatants. Protein concentration in each fraction was measured by the BCA assay [36].

2.8. FTSC labeling of protein carbonyls

Protein oxidation levels in plasma, liver and skeletal muscle were measured by a fluorescence-based assay as previously described [12,37,38]. Briefly, LIS or HIS protein fractions from liver, muscle and plasma samples were independently incubated with 1 mM FTSC in the dark (37°C, 2.5 h). FTSC specifically labels protein carbonyls. Afterward, proteins were precipitated with an equal volume of 20% chilled TCA (w/v) and centrifuged at 16,000*g* (20°C, 10 min). The pellets were washed five times with 100% ethanol/ethyl acetate (1:1) to remove the FTSC excess and finally redissolved in urea buffer (7 M urea, 2 M thiourea, 2% CHAPS, 0.5% Pharmalyte 3–10, 0.5% IPG 3–10 buffer and 0.4% DTT). FTSC-labeled proteins were stored at −80°C until use. Protein concentration was determined by Bradford assay [39].

2.9. Gel-electrophoresis-based evaluation of global and specific protein carbonylation levels

2.9.1. Gel electrophoresis and image analysis

To evaluate the effect of HFHS diets on protein carbonylation level, we used a proteomics approach based on gel electrophoresis [40]. In order to analyze global protein carbonylation, 30 μg of each FTSC-labeled sample were subjected to 1-D (monodimensional) SDS–polyacrylamide gel electrophoresis (PAGE) and run in a Mini-PROTEAN 3 cell (Bio-Rad, Hercules, CA). The analysis of carbonyl levels in specific proteins was performed by resolving FTSC-labeled proteins in two-dimensional (2-D) electrophoresis gel [12,38]. Briefly, 400 μg of protein was separated in 11-cm, pH 3–10, IPG strips (Immobiline DryStrip gels, GE Healthcare Science, Uppsala, Sweden) by using an Ettan IPGphor II isolectric focusing system (GE Healthcare Science) set at 20°C. After focusing, the strips were kept frozen at −80°C until use. The second dimension was performed in laboratory-made 10% SDS–polyacrylamide gels by using an Ettan Daltsix electrophoresis system (GE Healthcare Science) at 15°C. Two 11-cm IPG strips corresponding to both diets were run in the same 2-D electrophoresis gel (24 cm wide), and five gels were running in each assay.

FTSC-tagged proteins were visualized by exposing 1-D or 2-D gels to a UV transilluminator Molecular Imager Gel Doc XR System (Bio-Rad, Hercules, CA) equipped with a 520-nm band-pass filter (520DF30 62 mm). Then, gels were stained overnight with Coomassie dye PhastGel Blue R-350 (GE Healthcare Science) to visualize total protein level.

Image analysis of 1-D gels was performed with the 1-D gel analysis software LabImage 1D (Kapelan Bio-Imaging Solutions, Halle, Germany) on the basis of the overall optical volume per lane. Meanwhile, protein spots were detected and matched among 2-D gels by using the PDQuest software version 7.1 (Bio-Rad, Hercules). The intensity of the spots was expressed as parts per million of the total integrated optical density of the gel, which was approximately constant among gels.

2.9.2. Calculation of carbonylation indexes

To analyze the influence of diet on protein carbonylation level, we calculated a concentration-normalized "protein carbonylation index" as previously described [12,38] and compared that value between diets. This normalized parameter of carbonylation divides the fluorescence intensity of lane/band/spot in the FTSC-stained gel by the protein concentration represented by the intensity of Coomassie. Therefore, carbonylation index allows normalizing the protein carbonylation level (measured by FTSC intensity in gel) with protein abundance (measured by Coomassie intensity in gel) and offsetting possible differences in protein loading and protein concentration.

2.10. Identification of proteins by HPLC coupled with electrospray ionization ion trap MS/MS (LC-ESI-IT-MS/MS)

Spots corresponding to proteins of interest were excised from gels and digested *in situ* with sequencing-grade bovine trypsin according to a protocol previously described [41]. Protein identity was ascertained by an LC system model SpectraSystem P4000 (Thermo Scientific, San Jose, CA) coupled to an IT MS model LCQ Deca XP Plus or LTQ Velos Pro with ESI interface (Thermo Scientific). Tryptic peptides were separated on a BioBasic-18 RP column, 0.18 mm×150 mm, 5 μm (Thermo Scientific) using 0.5% aqueous acetic acid and in 80% acetonitrile as mobile phases A and B, respectively. A 90-min linear gradient from 5% to 60% B, at a flow rate of 1.5–1.7 μl/min, was used. Peptides were detected using survey scans from 350 to 1600 Da (2 μscans), followed by MS/MS scans (2 μscans) of the six most intense peaks using an isolation width of 1 Da and a normalized collision energy of 35%. Fragmented masses were set in dynamic exclusion for 30 s after the second fragmentation event, and singly charged ions were excluded from MS/MS analysis.

Protein identification was performed by homology of experimental MS/MS peak lists with theoretical MS/MS spectra contained in the *Rattus norvegicus* UniProtKB/Swiss-Prot database (28,855 sequences) released in October 2013 by using the Sequest HT search engine (Proteome Discoverer 1.4; Thermo Scientific, San Jose, CA). The following search criteria were applied: tryptic cleavage, up to two missed cleavage sites, and tolerances ±1.5 Da for precursor ions and ±0.8 Da for MS/MS fragment ions. Methionine oxidation and carbamidomethylation of cysteine were set as variable modifications. Also, up to 18 different carbonyl modifications of amino acids were searched as variable modifications. These carbonyl modifications resulted from the direct oxidation of side chains of amino acid residues (oxidation of histidine to 2-oxohistidine, oxidation of cysteine or serine to 3-oxoalanine, oxidation of threonine to 2-amino-3-ketobutiric, oxidation of proline to glutamic semialdehyde or 5-oxoproline, oxidation of arginine to glutamic semialdehyde and oxidation of tryptophan to 3-hydroxykynurenine, kynurenine, *N*-fomylkynurenine, hydroxy-*N*-fomylkynurenine) or the adduction with carbonyls derived from lipid peroxidation and glycoxidation by Michael and/or Schiff base addition (MDA, acrolein, crotonaldehyde, 4-oxo-2-nonenal, 2-hexenal, glyoxal, 4-hydroxy-2-nonenal, 4-hydroxy-2-hexenal, acetaldehyde). Since Sequest HT has the limitation of allowing just six modifications per search, several consecutive searches for each sample were required to explore oxidative sites of carbonyl modifications (Table 3 and Supplementary Tables S1 and S2). MS/MS spectra were manually inspected to identify an oxidation site and confirm the amino acid. The false discovery rate (FDR) was kept below 1%.

2.11. Statistical analysis

Single biological replicates for each dietary treatment, control (n=5) and HFHS (n=5), were subjected to three independent experiments of FTSC carbonyl labeling and gel electrophoresis. Therefore, 1-D and 2-D gels were performed at least three times for each type of protein fraction (LIS and HIS proteins) and biological sample (plasma, liver and skeletal muscle). Individual and global oxidation protein levels were reported as mean and standard deviation (S.D.). Statistical analysis was performed using the Student t test with Statistica 6.0 program (Statsoft, Inc., Tulsa, OK). The level of significant difference was set at P<.05.

3. Results

3.1. Metabolic changes induced by HFHS diet

No rat died in any group during the whole experimental period. The energy intake of HFHS rats was higher than controls throughout the experiment, rising to be approximately 24% higher since the ninth week, despite their lower food intake compared to controls (Table 1). This fact is explained by the much higher energy density of HFHS diet (4.7 kcal/g) in comparison to the control diet (2.9 kcal/g). The HFHS group significantly increased body, abdominal and liver fat weights. Thus, at the end of experimental period, HFHS rats weighed almost 28% more than control rats and showed about 52% more abdominal fat. Accordingly, rats fed HFHS exhibited an adiposity index significantly higher (34%) than control rats. Livers of HFHS rats accumulated also 3.8-fold more lipids than rats fed a control diet. Although not statistically significant, the hepatosomatic index of HFHS rats also tended to increase (Table 1). Additionally, HFHS diet elicited a significant effect on plasma insulin levels. Insulin concentrations were higher in rats fed HFHS diet than in control rats, and differences were significant from the fifth week on. Other parameters such as plasma glucose, HbA1c percentage, total

cholesterol, LDL and HDL cholesterol, and triglycerides did not change significantly between diets.

Histological features of the liver revealed hepatic steatosis and lobular inflammation in the group of HFHS animals (Fig. 1B, C and D). In contrast, rats fed control diet did not show a significant fat accumulation and inflammation in liver (Fig. 1A). No liver showed fibrosis.

In regards to the parameters associated to oxidative stress, Table 2 shows the level of lipid peroxidation, antioxidant enzyme activity and antioxidant capacity in plasma and liver. HFHS livers showed higher lipid peroxidation in terms of lipid hydroperoxides and conjugated dienes. However, plasma and liver MDA values did not change between diets.

The activity of the antioxidant enzymes SOD, CAT, GR and GPx, and the redox balance in terms of GSSG/GSH ratio were not different between dietary groups in both plasma and liver tissue. ORAC values also indicated no differences in the plasma and liver antioxidant capacity of rats fed control or HFHS diet.

3.2. Evaluation of protein oxidation in plasma

As evidenced in Fig. 2, long-term HFHS consumption triggered a significant increase of global protein carbonylation level in plasma. Fig. 2A shows total plasma proteins resolved on 1-D SDS-PAGE and stained with Coomassie blue. Fig. 2B shows plasma FTSC-labeled proteins resolved on 1-D gels. Graphical representation of global carbonylation indexes in plasma is included in Fig. 2C. Statistical analysis on individual protein bands revealed that the most abundant plasma protein was also the major protein target of oxidative damage according to its highest carbonylation level (Fig. 2D). This protein was successfully identified as serum albumin by MS/MS (P02770, Sequest HT score: 696.5) and constitutes approximately 55% of total plasma proteins [42]. In the HFHS group, albumin underwent an increase higher than 50% in carbonylation as compared to the control group, and that increment represented about 50% of the increase of total protein carbonylation in plasma from HFHS rats.

3.3. Evaluation of protein oxidation in skeletal muscle

Global protein carbonylation indexes were calculated for LIS and HIS fractions of skeletal muscle and respectively compared between diets (data not shown). These indexes were not significantly different between dietary groups, and therefore, there was not a significant effect of the high-caloric diet. However, some aspects of the carbonylated protein profiles should be highlighted (Supplementary Figs. S1 and S2). In the LIS muscular fraction, Coomassie-stained gels showed that proteins were mainly concentrated between ~45 and ~35 kDa (Supplementary Fig. S1A). However, the most carbonylated proteins were located at lower mass ranges (~40 and ~20 kDa) (Supplementary Fig. S1B). Thereby, we found high-concentrated, low-oxidized protein bands (as band 5) and low-concentrated, high-oxidized protein bands as band 9, and particularly band 10, for which carbonylation index was one order of magnitude higher to the rest of proteins (Supplementary Fig. S1C). Protein oxidation occurring in the HIS fraction appeared to be homogeneously distributed throughout mass and abundance protein ranges (Supplementary Fig. S2A and B), and their carbonylation indexes were in the same order of magnitude (Supplementary Fig. S2C).

3.4. Evaluation of protein oxidation in liver

The analysis of 1-D gels of liver LIS and HIS proteins showed significant differences in the global protein carbonylation levels of control and HFHS groups (Figs. 3 and 4). Interestingly, LIS and HIS proteins were significantly more carbonylated in the HFHS rats than control animals ($P<.05$ and $P<.001$, respectively). Similarly to plasma, liver proteins exhibited different susceptibility to the oxidative damage induced by HFHS diet, and such specific vulnerability was found in LIS and HIS fractions (Fig. 3, bands 1–6 and Fig. 4, bands 1–2). Thus, some particular proteins seemed to be targets of the carbonylation triggered by HFHS diet consumption.

To deepen the characterization of carbonylated proteins targeted by HFHS diets, 2-D gels were performed to isolate and identify individual proteins. Fig. 5A and B shows, respectively, LIS and HIS fractions resolved on 2-D gels. Only proteins displaying a significant change in their protein carbonylation level were marked in gels.

Seven protein spots from the LIS fraction displayed a significant change in carbonylation (Fig. 5A and Table 3). Six of them showed an increment of carbonylation in samples corresponding to HFHS diet (spots numbered as 1, 2, 3, 4, 5 and 6). Only one protein spot presented a reduced carbonylation level in the HFHS group (spot 7). MS/MS analysis revealed the following identifications: spot 1 was assigned to mitochondrial enzyme carbamoyl-phosphate synthase (ammonia) (CPSase1); spot 2 was identified as albumin; spot 3 was, in fact, a mixture of two different proteins; one was bifunctional adenosine triphosphate (ATP)-dependent dihydroxyacetone kinase/flavin adenine dinucleotide (FAD)-adenosine monophosphate (AMP) lyase (cyclizing), and other was CAT. Spot 4 was another mitochondrial enzyme, aldehyde dehydrogenase (ALDH2). Argininosuccinate synthetase (ASS) was comprised in spot 5. Spot 6 contained regucalcin, and finally, spot 7 was the mitochondrial aspartate transaminase (AST2).The analysis of 2-D HIS protein gels (Fig. 5B and Table 3) revealed four protein spots (numbered as 8, 9, 10 and 11) with increased carbonylation in rats fed a HFHS diet. Protein spot 8 was identified as the subunit beta of mitochondrial ATP synthase. Spot 9 was actin cytoplasmic 1. Two different proteins were mingled in spot 10: mitochondrial aldehyde dehydrogenase and 4-trimethylaminobutyraldehyde dehydrogenase. Finally, spot 11 was also a mitochondrial protein, glutamate dehydrogenase 1 (GDH1). Protein identifications and their cellular compartments are summarized in Table 3 and detailed in supplementary Tables S1 and S2. Two proteins were found in spot 3 and in spot 10. The efforts made using high-resolution isoelectric focusing strips (18cm) in order to resolve the two proteins were unsuccessful. Hence, it was impossible to know if the change in protein carbonylation was due to a single protein or both.

Further investigation was performed to identify oxidative sites and specific carbonyl modifications. Among the 13 proteins listed in Table 3, corresponding to the 11 spots of interest, all proteins except four of them (bifunctional ATP-dependent dihydroxyacetone kinase/FAD-AMP lyase, CAT, 4-trimethylaminobutyraldehyde dehydrogenase and ASS) demonstrated to have at least one oxidation site. Carbonylation sites found on each protein are shown in Table 3. It should be noted that all proteins exhibited proline residues oxidized (to glutamic semialdehyde and/or 5-oxoproline), with the exception of proteins found in spot 10. Moreover, ALDH2 (spots 4 and 10) and GDH1 (spot 11) showed carbonylation sites on tryptophan residues resulting from the oxidation of their side chain. Serine residues held carbonyl moieties arising from oxidation of the side chain as shown for serum albumin and ALDH2. Oxidation of arginine to glutamic semialdehyde was detected on two proteins: CPS1 and albumin. Finally, some oxidative modifications were detected on single carbonylated proteins: CPS1 showed carbonylation sites on threonine (from oxidation of its side chain), asparagine and cysteine residues (which were respectively bound to acetaldehyde and 2-hexenal); lysine residues bound to acrolein were found in AST2; and histidine residues were oxidized to 2-oxohistidine, forming a Schiff base adduct with acetaldehyde on cytoplasmic actin 1.

4. Discussion

The results presented here show that long-term consumption of a HFHS diet causes a characteristic carbonylation pattern in plasma and liver. Meanwhile, proteins from skeletal muscle are similarly carbonylated in animals fed HFHS and control diets. This characteristic map is in agreement with a previous study describing an

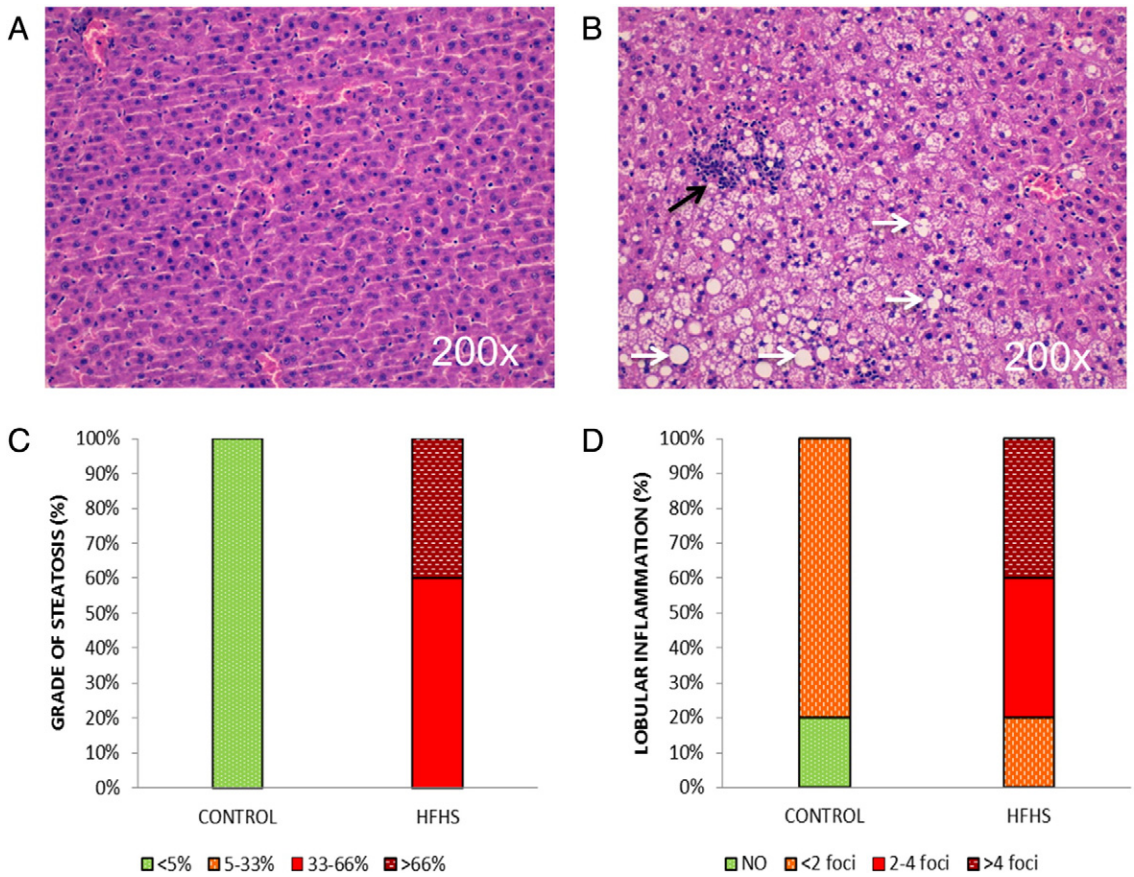

Fig. 1. Liver histology after hematoxylin/eosin staining of liver sections from a representative rat fed a (A) control diet (200×) and (B) HFHS diet (200×). Lobular inflammation cell infiltrations are marked with a black arrow, and steatosis is marked, in part, with white arrows. (C and D) The grade of steatosis and lobular inflammation, respectively, found in control and HFHS rats, both expressed as percentages.

increment of liver protein oxidation in HFHS diet-fed rats, while protein oxidation in skeletal muscle was not modified [17].

The distinctive protein oxidation found in the HFHS group occurred in parallel with a significant increase in abdominal and liver fat, body weight and insulin levels in plasma. Abdominal fat and insulin resistance are strongly related in humans [43], and insulin resistance plays also an important role in liver fat accumulation and inflammation [44]. Our results also indicate a higher lipid peroxidation in terms of hydroperoxides and conjugated dienes in livers from HFHS rats. This is in agreement to their elevated hepatic steatosis and inflammation, and previous correlations of an increased lipid peroxidation in animal models of nonalcoholic fatty liver disease (NAFLD) [45]. Thus, the increment of liver conjugated dienes and hydroperoxides found in the study can be related to hepatic steatosis and inflammation. The higher protein carbonylation and the increased production of primary and intermediary oxidation products did not correlate with the MDA values found in liver. Previous investigations had indicated that TBA reaction is not specific for the MDA generated by lipid peroxidation and that MDA analysis may have interferences in complex biological samples such as liver tissue [46,47].

In regard to antioxidant activities in liver, they did not show any significant differences between rats. This could be a consequence of

Table 2
Blood and liver oxidative stress parameters

	Plasma		Liver	
	Control (n=5)	HFHS (n=5)	Control (n=5)	HFHS (n=5)
Conjugated dienes (nmol/mg protein)			10.2 (0.9)	87.8 (30.3)**
Lipid hydroperoxides (mEq O_2/kg protein)			2.3 (0.3)	4.2 (0.6)**
MDA (nmol/mg protein)	0.2 (0.05)	0.2 (0.05)	0.5 (0.1)	0.6 (0.1)
SOD (U/g Hb or g tissue)	2112.2 (644.9)	2576.0 (1417.9)	13.6 (6.8)	14.5 (5.0)
CAT (mmol/(min·g Hb or g T))	116.2 (9.2)	119.3 (7.7)	10.3 (3.6)	11.1 (3.4)
GR (U/g Hb or g T)	0.4 (0.2)	0.2 (0.1)	8.8 (1.1)	7.4 (3.2)
GPx (U/g Hb or g T)	107.4 (9.9)	112.2 (10.6)	35.8 (4.1)	43.9 (17.5)
ORAC (mmol TE/L P or kg T)	10.3 (0.6)	8.6 (2.0)	18.6 (1.0)	15.4 (3.1)
GSSG/GSH			2.6 (0.3)	2.5 (0.7)

Results are means (standard deviation); n, number of rats.
Abbreviations: P, plasma; T, tissue; TE, Trolox equivalents.
** P<.01 vs. control group.

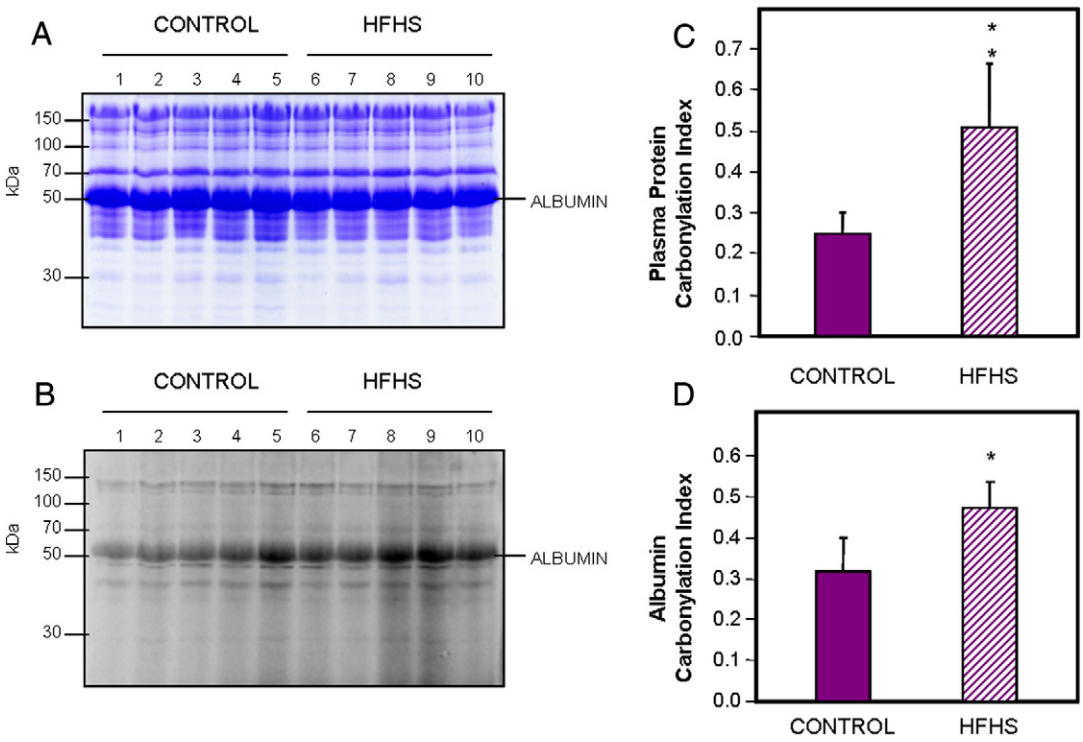

Fig. 2. Effect of HFHS diet on carbonylation level of plasma proteins from male Sprague–Dawley rats. (A) 1-D Coomassie-stained gel of fresh plasma proteins from control and HFHS dietary groups. Lanes 1, 2, 3, 4 and 5: control diet. Lanes 6, 7, 8, 9 and 10: HFHS diet. (B) 1-D FTSC-stained gel of fresh plasma proteins from control and HFHS dietary groups. Lanes 1, 2, 3, 4 and 5: control diet. Lanes 6, 7, 8, 9 and 10: HFHS diet. (C) Global plasma protein carbonylation index for control and HFHS dietary groups. Data are presented as mean±S.D. (D) Plasma albumin carbonylation index for control and HFHS dietary groups. Data are presented as mean±S.D. *P<.05, **P<.01.

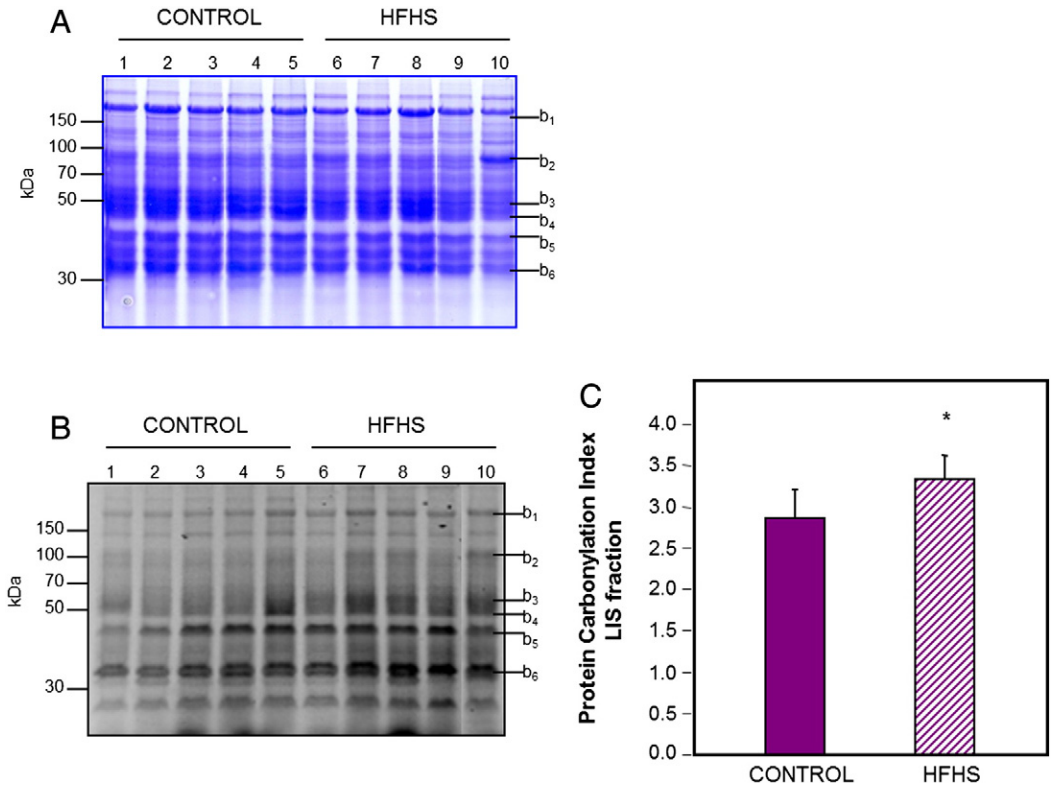

Fig. 3. Effect of HFHS diet on carbonylation level of LIS liver proteins from male Sprague–Dawley rats. (A) 1-D Coomassie-stained gel of LIS proteins from control and HFHS dietary groups. Lanes 1, 2, 3, 4 and 5: control diet. Lanes 6, 7, 8, 9 and 10: HFHS diet. (B) 1-D FTSC-stained gel of LIS proteins from control and HFHS dietary groups. Lanes 1, 2, 3, 4 and 5: control diet. Lanes 6, 7, 8, 9 and 10: HFHS diet. (C) Global LIS protein carbonylation index for control and HFHS dietary groups. Marked bands (b1 to b6) showed differential protein carbonylation index. Data are presented as mean±S.D. *P<.05.

metabolic adaptations of the liver to a prolonged high-caloric consumption as previously suggested [48].

Insulin resistance and protein carbonylation seem to be closely related through activation of c-jun NH(2)-terminal kinases by an increased protein carbonylation level [5,19]. On the contrary, plasma glucose values did not change between diets. This normoglycemia was coherent with the absence of change in the glycated hemoglobin percentage observed [49]. These results highlight the higher insulin level required in the HFHS group to maintain normal glucose levels compared to rats fed control diet; this is in turn the earliest sign of the onset of type 2 diabetes in HFHS rats [50].

Our results also showed that HFHS diet did not elevate plasma triglycerides and cholesterol levels. Similar plasma lipid profiles with different combinations of high caloric diets have been previously found [17,51,52], and several studies have even reported decreased plasma triglycerides and cholesterol levels [53–56]. Since it is well recognized that high refined sugar dietary content (up 60% of calories) can elevate plasma triglycerides levels [2,57], the level of sucrose in our diet was possibly too low (27.2% of calories) to produce a hypertriglyceridemic state. Moreover, an increase in triglyceride clearance by the adipose tissue and liver, evidenced in this work through the increase of weight and the liver steatosis and inflammation, may also contribute to maintain, or even to decrease, plasma triglycerides levels [51]. The high level of fat in our diet could tend to inhibit fatty acid synthesis [55]. This fact together with the low level of cholesterol in the HFHS diet (0.05%, from milk fat), which was possibly not enough to elevate cholesterol levels in plasma, may explain that HFHS feeding did not change cholesterol levels that even seemed to tend to lower concentrations. Previous studies have reported inconsistent data for the induction of hypercholesterolemia in rats by a pure high-fat diet without cholesterol added [58]. Successful dietary interventions aimed to achieve hypercholesterolemia currently incorporate high-caloric diets with more than 0.2% cholesterol [17,51,56].

The map of the characteristic carbonylation pattern of proteins can provide a new insight into the pathogenesis of metabolic diseases derived from the high consumption of fat and refined carbohydrate. We found that plasma albumin is a target of oxidative stress triggered by the intake of an HFHS diet rich in milk fat. Milk fat is composed mainly of triglycerides in which the main fatty acids are palmitate, stearate, oleate, linoleate and linolenate [59]. In a previous work, we demonstrated that omega-3 fatty acids of marine origin (eicosapentaenoic acid and docosahexaenoic acid), especially when given at 1:1 ratio, reduced plasma albumin oxidation — in comparison with other fatty acids, mainly α-linolenic acid from linseed oil and linoleic acid from soybean oil — in healthy rats [12]. It appears that the quantity and/or quality of dietary fat influences plasma albumin oxidation. Perhaps, the role of albumin as fatty acid transporter in plasma might explain this interdependence. The increased carbonylation of albumin, an important antioxidant in plasma [60], suggests that HFHS diet triggers oxidative stress and particularly oxidative damage on proteins. In accordance with this, Pandey et al. [61] noted that type-2 diabetic patients showed higher plasma carbonyl levels and more advanced oxidation protein products than healthy people, and these protein modifications were postulated to be among the molecular mechanisms leading to diabetic complications.

Liver profiles revealed that mitochondrial proteins are the main targets of the differential diet-induced carbonylation, highlighting the importance of subcellular localizations of the proteins. Four central proteins associated to nitrogen metabolism suffered significant

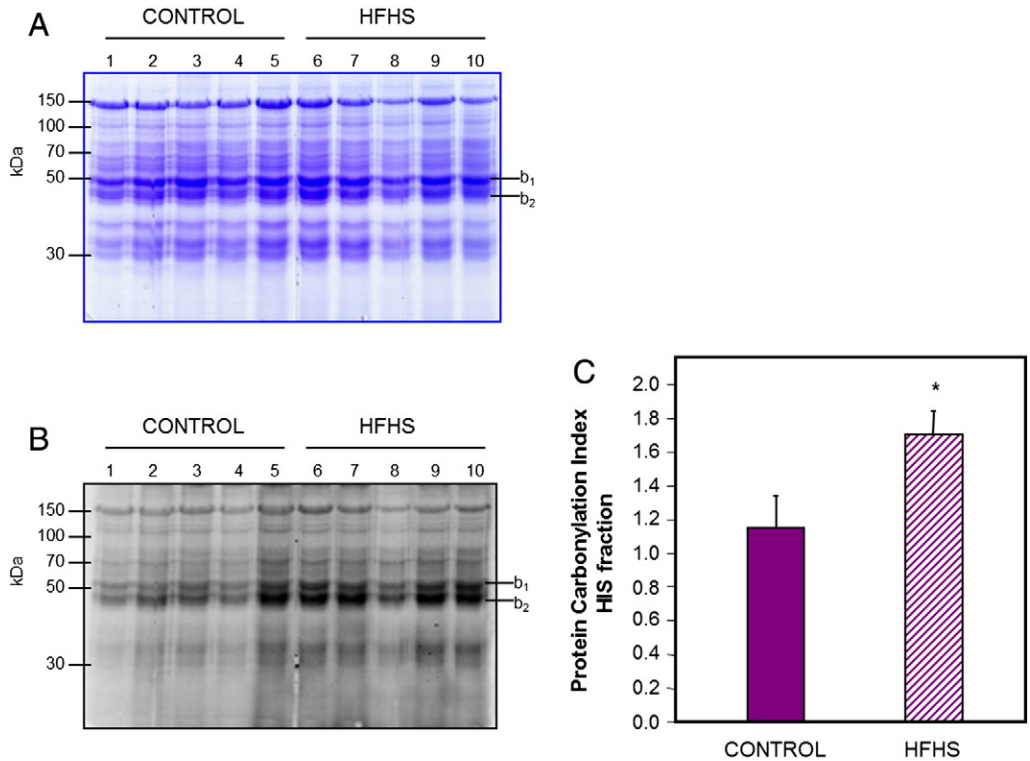

Fig. 4. Effect of HFHS diet on carbonylation level of HIS liver proteins from male Sprague–Dawley rats. (A) 1-D Coomassie-stained gel of HIS proteins from control and HFHS dietary groups. Lanes 1, 2, 3, 4 and 5: control diet. Lanes 6, 7, 8, 9 and 10: HFHS diet. (B) 1-D FTSC-stained gel of HIS proteins from control and HFHS dietary groups. Lanes 1, 2, 3, 4 and 5: control diet. Lanes 6, 7, 8, 9 and 10: HFHS diet. (C) Global HIS protein carbonylation index for control and HFHS dietary groups. Marked bands (b1 and b2) showed differencial protein carbonylation index. Data are presented as mean±S.D. *P<.05.

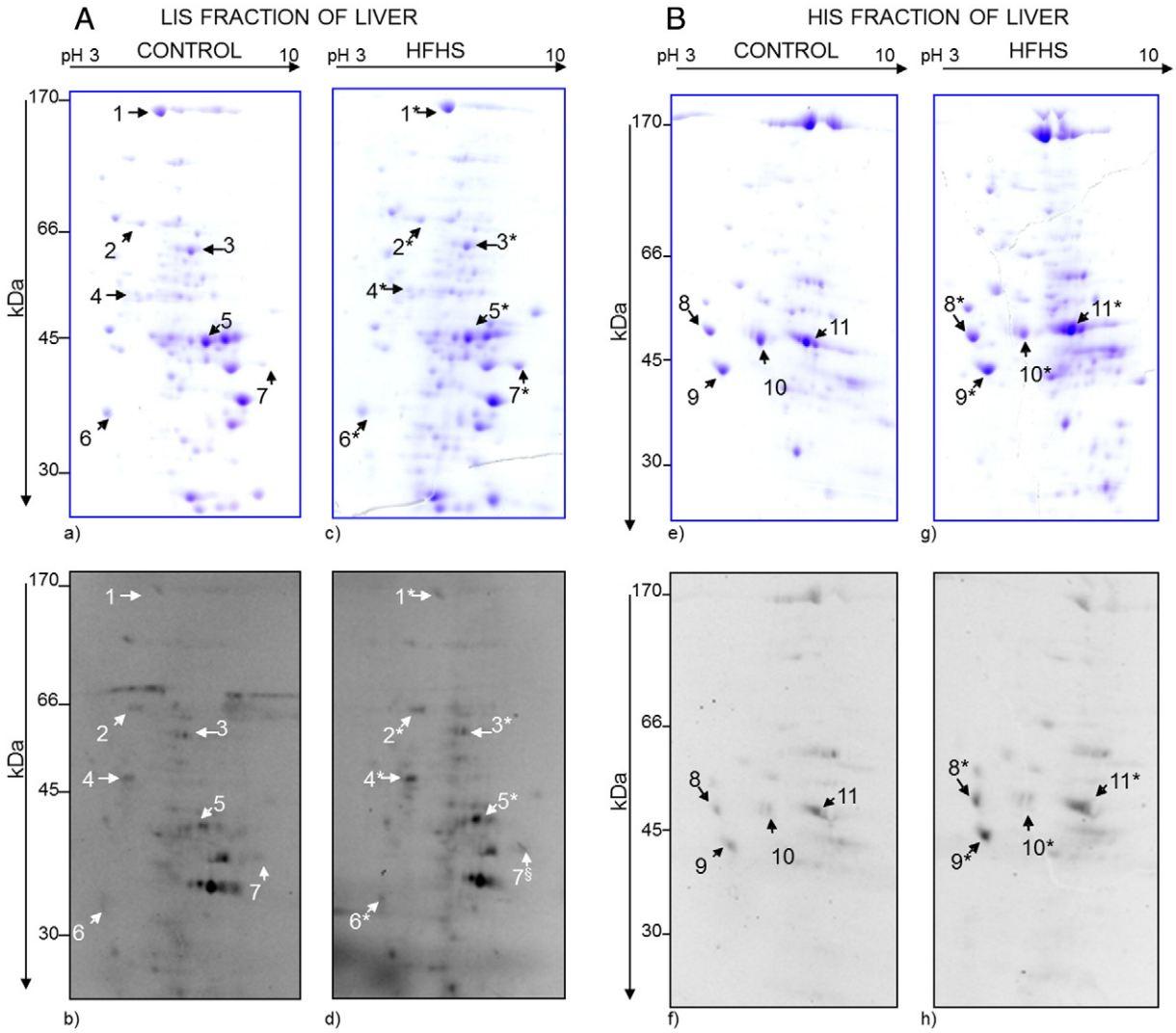

Fig. 5. Representative 2-D gels for control and HFHS groups showing total and carbonylated protein profiles of LIS and HIS liver fractions. Coomassie-stained 2-D gels that represent the abundance of LIS liver proteins in control and HFHS diets are shown respectively in panels (A) and (C). The level of carbonylation of LIS liver proteins in control and HFHS diets by visualizing images of the FTSC-stained 2-D gels is shown respectively in panels (B) and (D). The corresponding Coomassie-stained 2-D gels of HIS liver proteins from control and HFHS rats are shown respectively in panels (E) and (G). FTSC-stained 2-D gels of HIS liver proteins from control and HFHS rats are shown respectively in panels (F) and (H). *Proteins with higher carbonylation index (FTSC intensity normalized by the Coomassie intensity) in HFHS rats at $P<.05$. §Proteins with lower carbonylation index in HFHS rats at $P<.05$. Numbered protein spots represent carbonylated proteins confidently identified, and they are listed in Table 3.

oxidative transformations. CPSase1 and ASS (key enzymes from urea cycle) together with GDH1 were more carbonylated in the HFHS group. Only mitochondrial AST2 appeared less oxidized by HFHS diet. Such alterations can influence amino acid and protein metabolism. Consistent with this, Barber et al. [62] reported that the consumption of high-caloric diets, specifically, "cafeteria" diet, causes a decline in the activity of the enzymes of urea cycle. Interestingly, enzymatic activities of CPSase1 and ASS showed the most dramatic reduction. The level of CPSase1 also significantly decreased in a genetic rat model of obesity and type 2 diabetes [63]. A metabolomic study revealed that HFHS diet reduces plasma levels of nitrogen compounds, including urea [64]. Moreover, cafeteria-fed rats also showed high circulating amino acids levels [65]. Accordingly, mitochondrial GDH1 plays a central role in the catabolism of amino acids, particularly in the branched-chain amino acid (valine, leucine and isoleucine) catabolism [66]. The carbonylation observed for GDH1 in HFHS rats could contribute to explain the higher levels of amino acids in plasma as well as the reduced urea production caused by this kind of diets.

Unlike the rest of the identified proteins, the HFHS diet reduced the carbonylation level of the mitochondrial AST2, a multifunctional enzyme that plays a role in amino acid metabolism, and in urea and tricarboxylic acid cycles. Interestingly, AST2 was less oxidized in soybean-oil-fed rats compared to fish-oil-fed rats, just the opposite behavior to the other liver proteins which were more oxidized by soybean supplementation [12]. More investigation is needed to explain the impact of diet on AST2 carbonylation and the biological relevance of its differential behavior in terms of carbonylation.

Feillet-Coudray et al. [17] found lowered activities of the complex II and complexes II+III of the liver mitochondrial respiratory chain in HFHS-fed rats. Besides, our results suggest that ATP synthase (complex V) may lose activity due to its higher carbonylation in HFHS-fed rats. This fact could reduce oxidative phosphorylation and lower ATP cellular concentrations to finally result in mitochondrial disruption [67]. Supporting this hypothesis, Guo et al. [68] reported that the *in vitro* carbonylation of beta subunit of ATP synthase drastically decreases the enzyme activity. Moreover, lower ATP production due to reduction of oxidative phosphorylation could

Table 3
Identification of LIS and HIS liver proteins with different carbonylation levels between dietary groups

Spot no.	LIS/HIS fraction	Identification	Accession	Cellular component	Significant peptides (FDR<1%)	Sequence coverage (%)	Protein carbonylation index[a]		Oxidative modifications[b]
							Control (n=5)	HFHS (n=5)	
1	LIS	Carbamoyl-phosphate synthase (ammonia), mitochondrial	P07756	Mitochondrion	44	46.53	0.55 (0.21)	1.14 (0.44)*	^{1}N649, ^{1}N652 ^{4}C648 ^{5}T295, ^{5}T300 ^{6}P99, ^{6}P464, ^{6}P501, ^{6}P601 ^{7}R1039
2	LIS	Serum albumin	P02770	Cytoplasm	13	30.92	0.89 (0.42)	1.85 (0.82)*	^{6}P510 ^{7}R509 ^{8}S513
3	LIS	Bifunctional ATP-dependent dihydroxyacetone kinase/FAD-AMP lyase (cyclizing)	Q4KLZ6	Cytoplasm	5	9.86	1.38 (0.86)	3.33 (1.27)*	
		Catalase	P04762	Peroxisome	2	5.69			
4	LIS	Aldehyde dehydrogenase, mitochondrial	P11884	Mitochondrion	16	41.04	2.55 (1.11)	9.43 (6.51)*	^{6}P94 ^{8}S93 ^{10}W95 ^{11}P94
5	LIS	Argininosuccinate synthetase	P09034	Cytoplasm Outer mitochondrial membrane	5	13.59	0.41 (0.13)	0.74 (0.27)*	
6	LIS	Regucalcin	Q03336	Cytoplasm	5	24.75	0.31 (0.26)	1.15 (0.74)*	^{6}P124
7	LIS	Aspartate transaminase, mitochondrial	P00507	Mitochondrion	10	32.33	1.57 (0.52)	0.64 (0.22)*	^{2}K107 ^{6}P98 ^{11}P98
8	HIS	ATP synthase beta subunit	G3V6D3	Mitochondrion	23	69.19	0.83 (0.16)	1.48 (0.42)*	^{11}P131, ^{11}P333, ^{11}P396, ^{11}P400, ^{11}P503, ^{11}P512
9	HIS	Actin, cytoplasmic 1	P60711	Cytoplasm	8	42.93	0.84 (0.17)	1.37 (0.26)*	^{1}H275 ^{3}H73 ^{11}P70
10	HIS	Aldehyde dehydrogenase, mitochondrial	P11884	Mitochondrion	15	49.71	0.50 (0.22)	1.14 (0.31)*	^{9}W471
		4-trimethylaminobutyraldehyde dehydrogenase	Q9JLJ3	Cytoplasm	3	7.89			
11	HIS	Glutamate dehydrogenase 1, mitochondrial	P10860	Mitochondrion	16	42.11	0.45 (0.08)	0.62 (0.08)*	^{6}P224, ^{6}P340 ^{9}W338 ^{10}W338

Spots of interest were identified by LC-ESI-IT-MS/MS as described in the Section 2.10. Protein spot no. refers to the numbered spots in 2-D gels shown in Fig. 5. For each protein spot, different parameters are indicated: tissue liver fraction, cellular component, significant peptides (FDR<1%), % sequence coverage, protein carbonylation indexes and oxidative modifications found in each protein. Results are means (standard deviation); n, number of rats

[a] Protein carbonylation index: (FTSC/Coomassie intensities).

[b] 1: Schiff base adduct with acetaldehyde, 2: Michael-type adduct with acrolein, 3: 2-oxohistidine, 4: Michael-type adduct with 2-hexenal, 5: 2-amino-3-ketobutiric, 6: glutamic semialdehyde (P), 7: glutamic semialdehyde (R), 8: 3-oxoalanine (S), 9: kynurenine, 10: *N*-formylkynurenine, 11: 5-oxoproline.

* P<.05 vs. control group.

increase the accumulation of oxidized proteins by inhibiting the mitochondrial ATP-dependent proteases, specifically of the ATP-dependent Lon protease that is implicated in the removal of these oxidized proteins. [7,69]. Taking into consideration that the reduced mitochondrial enzyme activity precedes the development of NAFLD and insulin resistance [70], the higher level of mitochondrial enzyme carbonylation observed was consistent with the hyperinsulinemia and fatty liver developed by HFHS-fed rats.

Presumably, the higher carbonylation level of mitochondrial ALDH2 and regucalcin in HFHS-fed rats may accelerate the oxidative deterioration of hepatic cells because both enzymes are linked to the cellular antioxidant defense. ALDH2 is involved in the antioxidant defense against toxic lipid peroxidation carbonyls such as 4-hydroxy-2-nonenal [71], and enzymes belonging to the ALDH family are carbonylation targets in adipose tissue of obese and insulin-resistant mice [6]. Regucalcin has an activating effect on SOD [72] and a suppressive effect on nitric oxide synthase activity in liver cytosol [73]. Moreover, regucalcin appears to be a key molecule in lipid metabolic disorders and diabetes [74].

Finally, actin cytoplasmic 1 was significantly carbonylated in the HFHS group. Since actin is essential in the maintenance of cellular structure and functionality, its damage is associated with several diseases [75]. Thereby, HFHS-fed rats could potentially suffer filament disruption and functional losses.

The identification of the carbonylated sites on specific proteins strengthened the occurrence of oxidation in these proteins. At present, few carbonylation sites on proteins have been detected *in vivo*, and the potential impact of a certain oxidized amino acid found on a protein is not sufficiently known [76]. In this study, we found oxidized residues of proline, histidine, serine, arginine, asparagine, threonine, lysine and tryptophan in specific proteins. More research is needed to understand the individual significance of these carbonylated residues. Oxidative modifications can alter biological protein activity by increasing their propensity to cross-link and precipitation, causing difficulties in their degradation and enhancing their cellular toxicity. The identification of the carbonylated sites on proteins can be a good starting point to explain how specific carbonylated proteins affect biological systems and to make the use of oxidized proteins as disease markers in the future more likely.

To sum up, HFHS diet causes selective oxidative damage in proteins from different tissues. Results of this study indicate a different predisposition of plasma and liver proteins to suffer oxidative damage, being mitochondrial proteins the main targets of ROS attack. Some proteins (notably, albumin, CPSase1, ASS, GDH1, AST2, ALDH2, regucalcin, ATP synthase subunit beta, actin cytoplasmic 1) are the main targets of the ROS overproduced due to HFHS long-term consumption in the rat model. Given the huge importance and complexity of metabolic processes performed in the liver, this differential oxidative damage could contribute to explain how HFHS diets induce metabolic alterations leading to obesity, insulin resistance and NAFLD. Additionally, this protein carbonylation profile may be used in nutritional intervention studies as an early marker of diet induced metabolic disorders.

Supplementary data to this article can be found online at http://dx.doi.org/10.1016/j.jnutbio.2014.06.014.

Acknowledgments

This investigation has been supported by the Spanish Ministry of Science and Innovation (grants AGL2009-12374-C03-01, -02 and -03, IPT-2011-0828-90000, AGL2013-49079-C2-1,2-R). The Spanish Ministry of Science and Innovation is gratefully acknowledged for the doctoral fellowship to L.M. Xunta de Galicia and the European Social Fund are also thankfully recognized for the financial support of the postdoctoral "Isidro Parga Pondal" contract to M.P. EMT gratefully thanks the Panamanian government for a SENACYT / IFARHU predoctoral fellowship. L.M. also thanks the USC (Spain) for its doctoral program. The authors thank Lorena Barros and María Jesús González for their excellent technical assistance and AFAMSA (Vigo, Spain) for the provision of raw material.

References

[1] Dalle-Donne I, Giustarini D, Colombo R, Rossi R, Milzani A. Protein carbonylation in human diseases. Trends Mol Med 2003;9:169–76.
[2] Panchal SK, Brown L. Rodent models for metabolic syndrome research. J Biomed Biotechnol 2011;2011:351982.
[3] Brownlee M. Biochemistry and molecular cell biology of diabetic complications. Nature 2001;414:813–20.
[4] Maddux BA, See W, Lawrence JC, Goldfine AL, Goldfine ID, Evans JL. Protection against oxidative stress-induced insulin resistance in rat L6 muscle cells by micromolar concentrations of α-lipoic acid. Diabetes 2001;50:404–10.
[5] Ruskovska T, Bernlohr DA. Oxidative stress and protein carbonylation in adipose tissue — implications for insulin resistance and diabetes mellitus. J Proteomics 2013;92:323–34.
[6] Grimsrud PA, Picklo Sr MJ, Griffin TJ, Bernlohr DA. Carbonylation of adipose proteins in obesity and insulin resistance: identification of adipocyte fatty acid-binding protein as a cellular target of 4-hydroxynonenal. Mol Cell Proteomics 2007;6:624–37.
[7] Bulteau AL, Szweda LI, Friguet B. Mitochondrial protein oxidation and degradation in response to oxidative stress and aging. Exp Gerontol 2006;41:653–7.
[8] Stadtman ER, Levine RL. Protein oxidation. Ann N Y Acad Sci 2000;899:191–208.
[9] Davies MJ, Dean R. Radical-mediated protein oxidation: from chemistry to medicine. Oxford: Oxford Science Publications; 1997.
[10] Choi J, Malakowsky CA, Talent JM, Conrad CC, Gracy RW. Identification of oxidized plasma proteins in Alzheimer's disease. Biochem Biophys Res Commun 2002;293:1566–70.
[11] Himmelfarb J, McMonagle E. Albumin is the major plasma protein target of oxidant stress in uremia. Kidney Int 2001;60:358–63.
[12] Méndez L, Pazos M, Gallardo JM, Torres JL, Pérez-Jiménez J, Nogués R, et al. Reduced protein oxidation in Wistar rats supplemented with marine omega-3 PUFAs. Free Radic Biol Med 2013;55:8–20.
[13] Alisi A, Bruscalupi G, Pastore A, Petrini S, Panera N, Massimi M, et al. Redox homeostasis and posttranslational modifications/activity of phosphatase and tensin homolog in hepatocytes from rats with diet-induced hepatosteatosis. J Nutr Biochem 2012;23:169–78.
[14] Morrison CD, Pistell PJ, Ingram DK, Johnson WD, Liu Y, Fernandez-Kim SO, et al. High fat diet increases hippocampal oxidative stress and cognitive impairment in aged mice: implications for decreased Nrf2 signaling. J Neurochem 2010;114:1581–9.
[15] Dandona P, Mohanty P, Ghanim H, Aljada A, Browne R, Hamouda W, et al. The suppressive effect of dietary restriction and weight loss in the obese on the generation of reactive oxygen species by leukocytes, lipid peroxidation, and protein carbonylation. J Clin Endocrinol Metab 2001;86:355–62.
[16] Matsuzawa-Nagata N, Takamura T, Ando H, Nakamura S, Kurita S, Misu H, et al. Increased oxidative stress precedes the onset of high-fat diet-induced insulin resistance and obesity. Metabolism 2008;57:1071–7.
[17] Feillet-Coudray C, Sutra T, Fouret G, Ramos J, Wrutniak-Cabello C, Cabello G, et al. Oxidative stress in rats fed a high-fat high-sucrose diet and preventive effect of polyphenols: involvement of mitochondrial and NAD(P)H oxidase systems. Free Radic Biol Med 2009;46:624–32.
[18] Frohnert BI, Sinaiko AR, Serrot FJ, Foncea RE, Moran A, Ikramuddin S, et al. Increased adipose protein carbonylation in human obesity. Obesity 2011;19:1735–41.
[19] Yuzefovych LV, Musiyenko SI, Wilson GL, Rachek LI. Mitochondrial DNA damage and dysfunction, and oxidative stress are associated with endoplasmic reticulum stress, protein degradation and apoptosis in high fat diet-induced insulin resistance mice. PLoS One 2013;8:e54059.
[20] Bucolo G, David H. Quantitative determination of serum triglycerides by the use of enzymes. Clin Chem 1973;19:476–82.
[21] Young DS, Friedman RB. Effects of disease on clinical laboratory tests. Washington, DC: AACC Press; 2001.
[22] Sharp P, Rainbow S. Continuous glucose monitoring and haemoglobin A(1c). Ann Clin Biochem 2002;39:516–7.
[23] Bligh EG, Dyer WJ. A rapid method of total lipid extraction and purification. Can J Biochem Physiol 1959;37:911–7.
[24] Herbes SE, Allen CP. Lipid quantification of freshwater invertebrates: method modification for microquantitation. Can J Fish Aquat Sci 1983;40:1315–7.
[25] AOCS. Official and tentative methods of the American Oil Chemists' Society. 4th ed. Champain, IL: D Firestone. AOCS; 1989.
[26] Chapman RA, Mackay K. The estimation of peroxides in fats and oils by the ferric thiocyanate method. J Am Oil Chem Soc 1949;26:360–3.
[27] Mendes R, Cardoso C, Pestana C. Measurement of malondialdehyde in fish: a comparison study between HPLC methods and the traditional spectrophotometric test. Food Chem 2009;112:1038–45.
[28] Mateos R, Lecumberri E, Ramos S, Goya L, Bravo L. Determination of malondialdehyde (MDA) by high-performance liquid chromatography in serum and liver as a biomarker for oxidative stress: application to a rat model for hypercholesterolemia and evaluation of the effect of diets rich in phenolic antioxidants from fruits. J Chromatogr B 2005;827:76–82.
[29] Fukunaga K, Suzuki T, Takama K. Highly sensitive high-performance liquid chromatography for the measurement of malondialdehyde in biological samples. J Chromatogr 1993;621:77–81.
[30] Misra HP, Fridovich I. The role of superoxide anion in the autoxidation of epinephrine and a simple assay for superoxide dismutase. J Biol Chem 1972;247:3170–5.
[31] Cohen G, Dembiec D, Marcus J. Measurement of catalase activity in tissue extracts. Anal Biochem 1970;34:30–8.
[32] Wheeler CR, Salzman JA, Elsayed NM, Omaye ST, Korte Jr DW. Automated assays for superoxide dismutase, catalase, glutathione peroxidase, and glutathione reductase activity. Anal Biochem 1990;184:193–9.
[33] Hissin PJ, Hilf R. A fluorometric method for determination of oxidized and reduced glutathione in tissues. Anal Biochem 1976;74:214–26.
[34] Ou B, Hampsch-Woodill M, Prior RL. Development and validation of an improved oxygen radical absorbance capacity assay using fluorescein as the fluorescent probe. J Agric Food Chem 2001;49:4619–26.
[35] Taltavull N, Munoz-Cortes M, Lluis L, Jove M, Fortuno A, Molinar-Toribio E, et al. Eicosapentaenoic acid/docosahexaenoic acid 1:1 ratio improves histological alterations in obese rats with metabolic syndrome. Lipids Health Dis 2014;13:31.
[36] Smith PK, Krohn RI, Hermanson GT, Mallia AK, Gartner FH, Provenzano MD, et al. Measurement of protein using bicinchoninic acid. Anal Biochem 1985;150:76–85.
[37] Chaudhuri AR, de Waal EM, Pierce A, Van Remmen H, Ward WF, Richardson A. Detection of protein carbonyls in aging liver tissue: a fluorescence-based proteomic approach. Mech Ageing Dev 2006;127:849–61.
[38] Pazos M, da Rocha AP, Roepstorff P, Rogowska-Wrzesinska A. Fish proteins as targets of ferrous-catalyzed oxidation: identification of protein carbonyls by fluorescent labeling on two-dimensional gels and MALDI-TOF/TOF mass spectrometry. J Agric Food Chem 2011;59:7962–77.
[39] Bradford MM. A rapid and sensitive method for the quantitation of microgram quantities of protein utilizing the principle of protein-dye binding. Anal Biochem 1976;72:248–54.
[40] Laemmli UK. Cleavage of structural proteins during the assembly of the head of bacteriophage T4. Nature 1970;227:680–5.
[41] Jensen ON, Wilm M, Shevchenko A, Mann M. Sample preparation methods for mass spectrometric peptide mapping directly from 2-DE gels. In: Link AJ, editor. 2-D proteome analysis protocols. Totowa, NJ: Humana Press; 1998. p. 513–30.
[42] Anderson NL, Anderson NG. The human plasma proteome: history, character, and diagnostic prospects. Mol Cell Proteomics 2002;1:845–67.
[43] Carey DG, Jenkins AB, Campbell LV, Freund J, Chisholm DJ. Abdominal fat and insulin resistance in normal and overweight women: direct measurements reveal a strong relationship in subjects at both low and high risk of NIDDM. Diabetes 1996;45:633–8.
[44] Matteoni CA, Younossi ZM, Gramlich T, Boparai N, Liu YC, McCullough AJ. Nonalcoholic fatty liver disease: a spectrum of clinical and pathological severity. Gastroenterology 1999;116:1413–9.
[45] Lieber CS, Leo MA, Mak KM, Xu Y, Cao Q, Ren C, et al. Model of nonalcoholic steatohepatitis. Am J Clin Nutr 2004;79:502–9.
[46] Devasagayam TP, Boloor KK, Ramasarma T. Methods for estimating lipid peroxidation: an analysis of merits and demerits. Indian J Biochem Biophys 2003;40:300–8.

[47] Janero DR. Malondialdehyde and thiobarbituric acid-reactivity as diagnostic indices of lipid peroxidation and peroxidative tissue injury. Free Radic Biol Med 1990;9:515–40.
[48] Kučera O, Garnol T, Lotková H, Staňnkováa P, Mazurová Y, Hroch M, et al. The effect of rat strain, diet composition and feeding period on the development of a nutritional model of non-alcoholic fatty liver disease in rats. Physiol Res 2011;60: 317–28.
[49] Sikaris K. The correlation of hemoglobin A1c to blood glucose. J Diabetes Sci Technol 2009;3:429–38.
[50] Weir GC, Bonner-Weir S. Five stages of evolving beta-cell dysfunction during progression to diabetes. Diabetes 2004;53:S16–21.
[51] Yang Z-H, Miyahara H, Takeo J, Katayama M. Diet high in fat and sucrose induces rapid onset of obesity-related metabolic syndrome partly through rapid response of genes involved in lipogenesis, insulin signalling and inflammation in mice. Diabetol Metab Syndr 2012;4:32.
[52] Boqué N, Campión J, Paternain L, García-Díaz DF, Galarraga M, Portillo MP, et al. Influence of dietary macronutrient composition on adiposity and cellularity of different fat depots in Wistar rats. J Physiol Biochem 2009;65:387–95.
[53] Chalkley SM, Hettiarachchi M, Chisholm DJ, Kraegen EW. Long-term high-fat feeding leads to severe insulin resistance but not diabetes in Wistar rats. Am J Physiol Endocrinol Metab 2002;282:E1231–8.
[54] Lomba A, Milagro FI, García-Díaz DF, Marti A, Campión J, Martínez JA. Obesity induced by a pair-fed high fat sucrose diet: methylation and expression pattern of genes related to energy homeostasis. Lipids Health Dis 2010;9:60.
[55] Hallfrisch J, Cohen L, Reiser S. Effects of feeding rats sucrose in a high fat diet. J Nutr 1981;111:531–6.
[56] Yamamoto Y, Oue E. Antihypertensive effect of quercetin in rats fed with a high-fat high-sucrose diet. Biosci Biotechnol Biochem 2006;70:933–9.
[57] Angelova P, Boyadjiev N. A review on the models of obesity and metabolic syndrome in rats. TJS 2013;1:5–12.
[58] Buettner R, Schölmerich J, Bollheimer LC. High-fat diets: modeling the metabolic disorders of human obesity in rodents. Obesity 2007;15:798–808.
[59] Jensen RG, Ferris AM, Lammi-Keefe CJ. The composition of milk fat. J Dairy Sci 1991;74:3228–43.
[60] Halliwell B. Albumin — an important extracellular antioxidant? Biochem Pharmacol 1988;37:569–71.
[61] Pandey KB, Mishra N, Rizvi SI. Protein oxidation biomarkers in plasma of type 2 diabetic patients. Clin Biochem 2010;43:508–11.
[62] Barber T, Vina JR, Vina J, Cabo J. Decreased urea synthesis in cafeteria-diet-induced obesity in the rat. Biochem J 1985;230:675–81.
[63] Rector RS, Thyfault JP, Uptergrove GM, Morris EM, Naples SP, Borengasser SJ, et al. Mitochondrial dysfunction precedes insulin resistance and hepatic steatosis and contributes to the natural history of non-alcoholic fatty liver disease in an obese rodent model. J Hepatol 2010;52:727–36.
[64] Etxeberria U, de la Garza AL, Martínez JA, Milagro FI. Diet-induced hyperinsulinemia differentially affects glucose and protein metabolism: a high-throughput metabolomic approach in rats. J Physiol Biochem 2013;69:613–23.
[65] Rafecas I, Esteve M, Fernández-López JA, Remesar X, Alemany M. Individual amino acid balances in young lean and obese Zucker rats fed a cafeteria diet. Mol Cell Biochem 1993;121:45–58.
[66] Islam MM, Nautiyal M, Wynn RM, Mobley JA, Chuang DT, Hutson SM. Branched-chain amino acid metabolon: interaction of glutamate dehydrogenase with the mitochondrial branched-chain aminotransferase (BCATm). J Biol Chem 2010;285: 265–76.
[67] Pieczenik SR, Neustadt J. Mitochondrial dysfunction and molecular pathways of disease. Exp Mol Pathol 2007;83:84–92.
[68] Guo J, Prokai-Tatrai K, Nguyen V, Rauniyar N, Ughy B, Prokai L. Protein targets for carbonylation by 4-hydroxy-2-nonenal in rat liver mitochondria. J Proteomics 2011;74:2370–9.
[69] Bota DA, Ngo JK, Davies KJ. Downregulation of the human Lon protease impairs mitochondrial structure and function and causes cell death. Free Radic Biol Med 2005;38:665–77.
[70] Erjavec N, Bayot A, Gareil M, Camougrand N, Nystrom T, Friguet B, et al. Deletion of the mitochondrial Pim1/Lon protease in yeast results in accelerated aging and impairment of the proteasome. Free Radic Biol Med 2013;56:9–16.
[71] Yoon M, Madden MC, Barton HA. Developmental expression of aldehyde dehydrogenase in rat: a comparison of liver and lung development. Toxicol Sci 2006;89:386–98.
[72] Fukaya Y, Yamaguchi M. Regucalcin increases superoxide dismutase activity in rat liver cytosol. Biol Pharm Bull 2004;27:1444–6.
[73] Yamaguchi M, Takahashi H, Tsurusaki Y. Suppressive role of endogenous regucalcin in the enhancement of nitric oxide synthase activity in liver cytosol of normal and regucalcin transgenic rats. J Cell Biochem 2003;88:1226–34.
[74] Yamaguchi M, Murata T. Involvement of regucalcin in lipid metabolism and diabetes. Metabolism 2013;62:1045–51.
[75] Dalle-Donne I, Rossi R, Giustarini D, Gagliano N, Lusini L, Milzani A, et al. Actin carbonylation: from a simple marker of protein oxidation to relevant signs of severe functional impairment. Free Radic Biol Med 2001;31:1075–83.
[76] Madian AG, Regnier FE. Proteomic identification of carbonylated proteins and their oxidation sites. J Proteome Res 2010;9:3766–80.